

Synthesis of Sb(VO₃)₃ and study of ternary system $x\text{NH}_4\text{VO}_3 + (1 - x)(\text{NH}_4)_2\text{HPO}_4 + \text{Sb}_2\text{O}_3$

P. Melnikov · R. V. Gonçalves · H. Wender

Received: 31 August 2010/Accepted: 17 March 2011/Published online: 30 March 2011
© Akadémiai Kiadó, Budapest, Hungary 2011

Abstract Sb(VO₃)₃ has been synthesized by interaction between NH₄VO₃ and Sb₂O₃. The compound crystallizes in monoclinic system with lattice parameters: $a = 17.150$; $b = 15.940$ Å and angle $\beta = 90.50^\circ$. The scanning electronic microscopy shows thin flat plates measuring ~ 20 μm along with detritus material. The synthesis was simulated by thermal analysis and the final product identified by X-ray diffraction. Thermal analyses of the ternary system $x\text{NH}_4\text{VO}_3 + (1 - x)(\text{NH}_4)_2\text{HPO}_4 + \text{Sb}_2\text{O}_3$ lead to the formation of Sb(VO₃)₃ and SbPO₄ at 500 °C. At high temperature (900 °C), SbVO₄, SbOPO₄, VO and SbP₅O₁₄ are formed. The data of thermal analysis match with the composition of intermediate and final products. No solid solutions containing simultaneously PO₄³⁻ and VO₄³⁻ ions have been found.

Keywords Ammonium metavanadate · Ammonium hydrogen phosphate · Antimony oxide · Antimony metavanadate

Introduction

Currently, vanadium mixed oxides are well known as important materials due to the peculiarities of their physical

and chemical properties and their potential uses in a variety of applications, such as electrochemical devices [1], lithium microbatteries [2], photocatalysis [3], and sensors [4]. Vanadium antimonate (or antimony vanadate, depending on experimental conditions), in particular, is known for its high performance in catalytic reactions of oxidation and ammonoxidation [5]. The most characteristic feature of the systems containing vanadium and antimony is their lability because of the small differences between ionization potentials corresponding to V³⁺, V⁴⁺, and V⁵⁺ valence states. The compounds belonging the system Sb₂O₃–V₂O₅ readily and continually undergo redox transformations even in sealed tubes or in inert atmosphere [6]. That is why a number of stoichiometric and non-stoichiometric compounds such as VSbO₄, Sb₂V₂O₉, VSb_{1-y}O_{4-2y}, Sb_{1-y}V_{1-y}O₄, and SbVO₅ could have been obtained [7–9]. Nevertheless, no certain knowledge is available so far as to the existence of antimony metavanadate, Sb(VO₃)₃, which in the domain of phosphorus chemistry would manifest similarity with antimony polyphosphate, Sb(PO₃)₃ as its analog [10]. Surprisingly, Sb(VO₃)₃ has not been found even in the vanadium-rich region of the system Sb₂O₃–V₂O₅, when vanadium pentoxide, V₂O₅ was used as starting reagent [8]. However, there are all structural grounds to believe that this compound can exist and that ammonium metavanadate NH₄VO₃ may be a better candidate as vanadium donor for its preparation. Moreover, the parallel usage of ammonium hydrogen phosphate, (NH₄)₂HPO₄ along with NH₄VO₃ can help make clear the possibility of phosphorus replacement by vanadium with the formation of solid solutions. The aim of this work is the synthesis of the antimony metavanadate Sb(VO₃)₃ and the study of the phases forming in the ternary system $x\text{NH}_4\text{VO}_3 + (1 - x)(\text{NH}_4)_2\text{HPO}_4 + \text{Sb}_2\text{O}_3$ during thermal treatment.

P. Melnikov (✉)
Department of Clinical Surgery, School of Medicine,
Federal University of Mato Grosso do Sul, Caixa Postal 549,
Campo Grande, Mato Grosso do Sul, Brazil
e-mail: petrmelnikov@yahoo.com

R. V. Gonçalves · H. Wender
Physics Institute, Federal University of Rio Grande do Sul,
Bento Gonçalves Avenue, 9500, P.O. Box 15051,
91501-970 Porto Alegre, Brazil

Experimental

Ammonium metavanadate NH_4VO_3 and antimony (III) oxide Sb_2O_3 , both of analytical grade purity, from Fluka were used as starting reagents for the preparation of antimony metavanadate (batch A). Ammonium hydrogen phosphate $(\text{NH}_4)_2\text{HPO}_4$ (99.0% purity, from Synth) was additionally used as phosphorus donor for the study of the intermediate compounds containing both phosphorus and vanadium. The amount of phosphorus introduced was calculated using the expression $x\text{NH}_4\text{VO}_3 + (1 - x)(\text{NH}_4)_2\text{HPO}_4 + \text{Sb}_2\text{O}_3$, where $x = 0.1\text{--}0.9$ (batch B). The powders were ground in agate mortar and heated in a platinum crucible with a heating rate of $15\text{ }^\circ\text{C min}^{-1}$ up to 500 and $900\text{ }^\circ\text{C}$, separately. Then they were maintained at these plateaux for 120 min under ambient pressure and let cool spontaneously.

Thermal behavior was studied by thermal gravimetric analysis (TG) using a 50H Shimadzu instrumentation. Preparations were simulated by mixing up the above-mentioned starting materials and heating the test specimens (4–6 mg) at the rate of $15\text{ }^\circ\text{C min}^{-1}$ up to $900\text{ }^\circ\text{C}$ in the synthetic air flux. Mass losses during heating were measured and compared to previously expected values. X-ray diffraction (XRD) patterns were registered using a Siemens Kristalloflex diffractometer with a graphite diffracted beam monochromator and Ni filter. Scanning electron microscopy (SEM) and energy dispersive X-ray spectroscopy (EDS) were performed in a JEOL-JSM 5800 equipment. The compounds separately prepared in static conditions were identified by comparison of experimental X-ray patterns with available database files of the International Centre for Diffraction Data (ICDD).

Results and discussion

Synthesis of antimony metavanadate

Figure 1 shows a representative TG curve of the batch A. The mass losses at different stages of the treatment are always referred to the initial sum of $\text{NH}_4\text{VO}_3 + \text{Sb}_2\text{O}_3$. Three net mass losses can be seen at 194, 240, and $318\text{ }^\circ\text{C}$. The molecular mass of a minimal unit (either NH_3 or H_2O) capable to be eliminated separately is of 17–18 Da. On the other hand, since a single mol of metavanadate would not produce mass loss less than 15.7%, the existence of smaller experimental losses of 8.7 and 12.2% clearly indicate that a condensation process is taking place; most probably with the formation of bridges V–O–V. As the process has topotactic character with NH_3 trapped within V_2O_5 crystal lattice in varying quantities [11] the formation of strictly stoichiometric compositions for this interval has never been proved beyond reasonable doubt [12, 13].

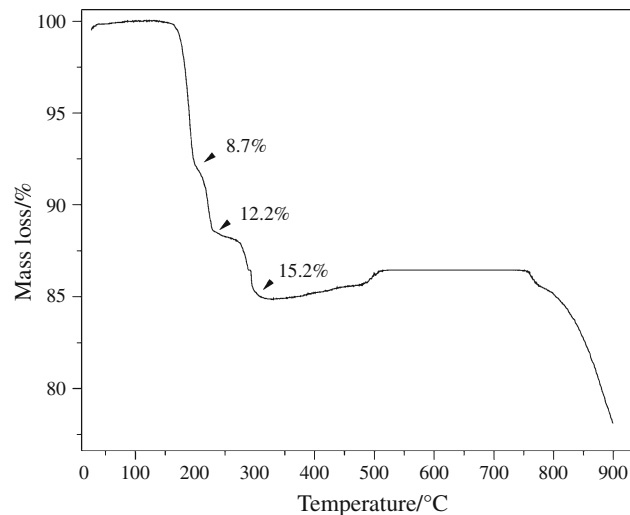
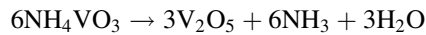


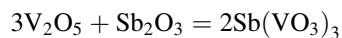
Fig. 1 TG curve simulating preparation of $\text{Sb}(\text{VO}_3)_3$

Yet the third experimental mass loss of 15.2% completes the elimination of volatile components, in agreement with the value 15.7% corresponding to the formation of vanadium pentoxide V_2O_5 :



At this early stage no reaction with the participation of Sb_2O_3 is taking place.

It is to be noted that TG curves at this level are labile due to the low kinetics of V_2O_5 crystallization and to the mutual exchange transformations $\text{V}^{5+} \leftrightarrow \text{V}^{3+}$ and $\text{Sb}^{3+} \leftrightarrow \text{Sb}^{5+}$. At this step some quantities of non-stoichiometric amorphous $\text{VSbO}_{4.5}$ (or $\text{V}_2\text{Sb}_2\text{O}_9$) are formed due to the electron hopping between V^{4+} and V^{5+} ions [8]. The resulting excess in oxygen explains a small (<1%) mass gain starting at $\sim 435\text{ }^\circ\text{C}$. At higher temperatures, remaining vanadium pentoxide reacts with antimony oxide giving antimony metavanadate:



The TG curve shows no losses because at this stage no volatile compounds are produced and consequently no mass loss could be expected. A clearly visible decrease of mass starts at the temperatures over $750\text{ }^\circ\text{C}$ caused, in all probability, by the metavanadate decomposition accompanied by the fast sublimation of V_2O_5 as in the case of well-known analogous phosphates [14].

X-ray diffraction pattern of the sample obtained during static heating at $500\text{ }^\circ\text{C}$ for 2 h is presented in Fig. 2. The set of interplanar distances and corresponding intensities is individual. No reflexions of either starting materials or vanadium antimonate are observed. The indexing of the X-ray pattern (Table 1) was successfully done on a monoclinic (pseudoorthorhombic) cell with the following

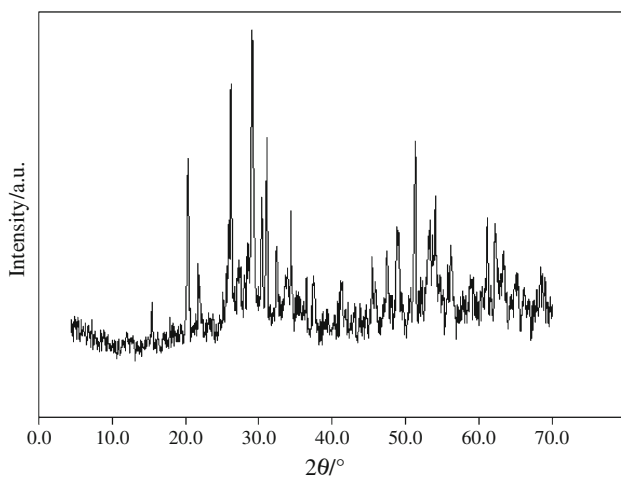


Fig. 2 X-ray diffractogram of $\text{Sb}(\text{VO}_3)_3$

Table 1 Indexing of antimony metavanadate

<i>h k l</i>	<i>d</i> _{calc.}	<i>d</i> _{obs.}	Intensity
3 0 0	5.716	5.716	14
3 1 -2	4.348	4.348	60
2 1 3	4.076	4.076	25
3 2 -2	3.931	3.931	09
3 1 3	3.594	3.594	16
1 4 -2	3.430	3.430	38
3 2 -3	3.372	3.372	83
4 3 -1	3.257	3.257	26
1 5 1	3.063	3.063	100
2 5 -1	2.929	2.929	44
4 4 -1	2.865	2.865	66
2 0 5	2.756	2.756	31
6 2 -1	2.649	2.649	24
5 4 0	2.599	2.599	42
1 3 -5	2.533	2.533	17
6 3 1	2.477	2.477	12
5 4 -2	2.454	2.454	22
7 1 1	2.385	2.385	22
6 2 -3	2.362	2.362	07
2 7 -1	2.177	2.177	20
1 1 -7	2.055	2.055	07
6 2 -5	1.986	1.986	28
6 3 -5	1.913	1.913	31
2 3 -7	1.896	1.896	34

parameters: $a = 17.150$; $b = 15.940$; $c = 14.600$ Å and angle $\beta = 90.50^\circ$. The coincidence in the values of the experimental and calculated interplanar distances is remarkable (Table 1). As can be easily seen, this lattice bears no similarities to the pattern of antimony polyphosphate $\text{Sb}(\text{PO}_3)_3$ [9], but this fact does not seem to be

surprising as polyanions like $[\text{PO}_3]_{3\infty}$ and $[\text{VO}_3]_{3\infty}$ are capable of displaying a vast variety of conformations [14].

As to the $\text{Sb}(\text{VO}_3)_3$ morphology, scanning electronic microscopy allows to see large compact blocks measuring ~ 20 µm. They are composed of thin flat plates clearly seen at the split right edge of the piece shown in Fig. 3. Loose small crystallites (~ 2 µm) resulting directly from blocks disintegration are spread over the surface. The mapping of vanadium, antimony, and oxygen performed by EDS offers evidence of high homogeneity, thus corroborating to the concept of a single metavanadate phase. These images are not presented here because of their poor resolution in black and white.

Study of ternary system $x\text{NH}_4\text{VO}_3 + (1 - x)(\text{NH}_4)_2\text{HPO}_4 + \text{Sb}_2\text{O}_3$

The TG curves of the batches B, that is $x\text{NH}_4\text{VO}_3 + (1 - x)(\text{NH}_4)_2\text{HPO}_4 + \text{Sb}_2\text{O}_3$, are given in Fig. 4 for $x = 0.1\text{--}0.9$. The mass losses till 400 °C quantitatively reflect the

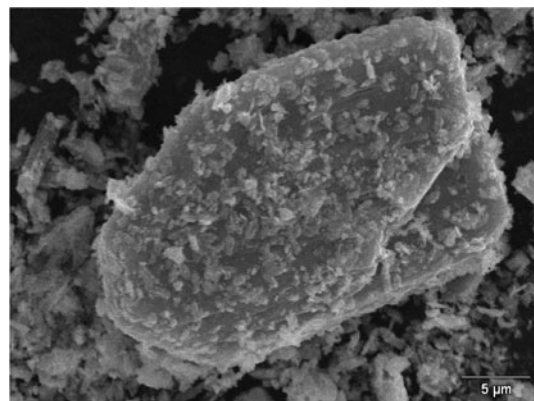


Fig. 3 Representative SEM image of $\text{Sb}(\text{VO}_3)_3$

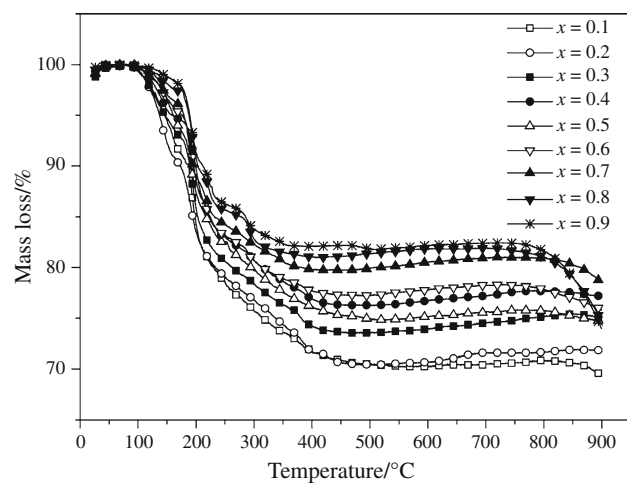
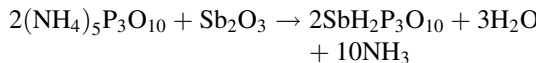


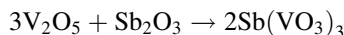
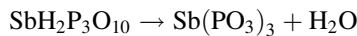
Fig. 4 TG curves of batches B for $x = 0.1\text{--}0.9$

elimination of water and ammonia as a result of thermal decomposition of both NH_4VO_3 giving V_2O_5 [12, 13] and $(\text{NH}_4)_2\text{HPO}_4$, giving ammonium tripolyphosphate $(\text{NH}_4)_5\text{P}_3\text{O}_{10}$ [15]. As in the case of $\text{Sb}(\text{VO}_3)_3$, up to this temperature, the antimony oxide remains intact within the batch.

After 400 °C, ammonium tripolyphosphate $(\text{NH}_4)_5\text{P}_3\text{O}_{10}$ reacts with Sb_2O_3 . As a result, five ammonium ions are replaced by an ion of antimony (III) and two protons, forming the acid antimony tripolyphosphate $\text{SbH}_2\text{P}_3\text{O}_{10}$ [16]. These mass losses fit the following reaction scheme:



As can be seen, acidic polyphosphate $\text{SbH}_2\text{P}_3\text{O}_{10}$ and polyphosphate monohydrate $\text{Sb}(\text{PO}_3)_3 \cdot \text{H}_2\text{O}$ have identical composition and therefore can be regarded as a rare case of inorganic isomers. Later, $\text{Sb}(\text{PO}_3)_3 \cdot \text{H}_2\text{O}$ loses one water molecule, forming antimony polyphosphate, as early described. At the same time, the previously formed vanadium pentoxide reacts with remaining antimony oxide to give antimony metavanadate $\text{Sb}(\text{VO}_3)_3$, according to the schemes:



The calculated and experimental mass losses of batch B up to 500 °C are presented in Table 2. They correspond to the above reaction schemes.

A set of diffraction patterns corresponding to the batches B after heating at 500 °C can be seen in Fig. 5. The crystalline phases corresponding to x from 0.3 to 0.9 were identified as $\text{Sb}(\text{VO}_3)_3$, varying only in the relative intensities of reflections, most probably due to the texture effects. There was no linear or otherwise evolution in lattice parameters, meaning that no substitution $\text{V} \rightarrow \text{P}$ had taken place. Taking into account that vanadium ion radius for the coordination IV (0.355 Å) is twice as great as that

Table 2 Experimental and calculated mass losses up to 500 °C for batches B

X	Found/%	Calculated/%
0.9	17.8	17.9
0.8	19.0	19.8
0.7	20.4	21.6
0.6	22.7	23.3
0.5	25.0	25.1
0.4	24.2	26.9
0.3	26.8	28.7
0.2	29.8	30.4
0.1	29.6	32.1

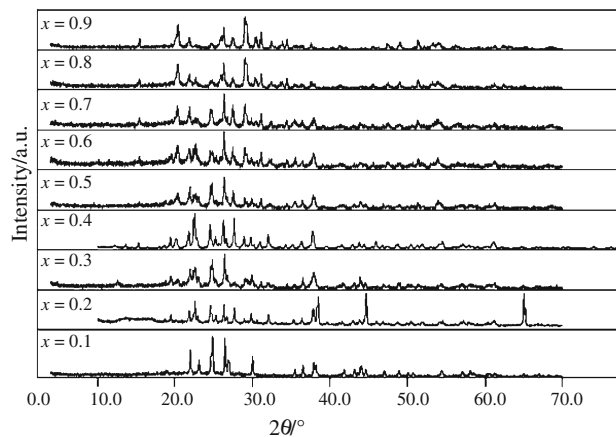


Fig. 5 XRD for batches B ($x = 0.1\text{--}0.9$) after heating at 500 °C

of phosphorus (0.17 Å) for the same coordination, it is reasonable to discard the formation of anionic solid solutions.

According to the proposed scheme, one also would expect the presence of antimony polyphosphate in growing quantities. However, this compound is usually available in its stable amorphous form, as the crystallization rarely occurs spontaneously [10]. Furthermore, viscous $\text{Sb}(\text{PO}_3)_3$ delays the vaporization of V_2O_5 ; that is why a net mass loss on TG curves is observed only for larger x (0.8 and 0.9) (Fig. 4).

As to the samples with $x = 0.1$ and 0.2, the major crystalline phase present is the SbPO_4 (ICDD 71-2275), probably because of the very small amount of vanadium compound diluted in these mixtures. Therefore, there are reflections not belonging to the SbPO_4 set, what should be due to the parallel formation of antimony ultraphosphate, a possibility that will be discussed later.

As to the behavior of the batches B after static heating at 900 °C for all values of x studied, one cannot draw conclusive results because of the complexity of the compositions. Here we limit ourselves with only the identifications of the crystalline phase or phases present formed at high temperature. The diffractograms can be subdivided into five groups. Figure 6 and Table 3 show diffraction patterns and the results of phase analysis.

First group: $x = 0.8$ and 0.9

X-ray diffraction patterns of the samples with $x = 0.8$ and 0.9 showed no differences. As can be seen in Fig. 6, they contain a single phase of tetragonal vanadium antimonate SbVO_4 , with lattice parameters $a = 4.598$ and $c = 3.078$ Å (ICDD 76-0678). The presence of SbVO_4 in these compositions, rich in vanadium, can be due to the oxidation of antimony to Sb^{5+} with simultaneous reduction of vanadium V^{5+} to V^{3+} at high temperatures [17]. There is no evidence of other crystalline phases.

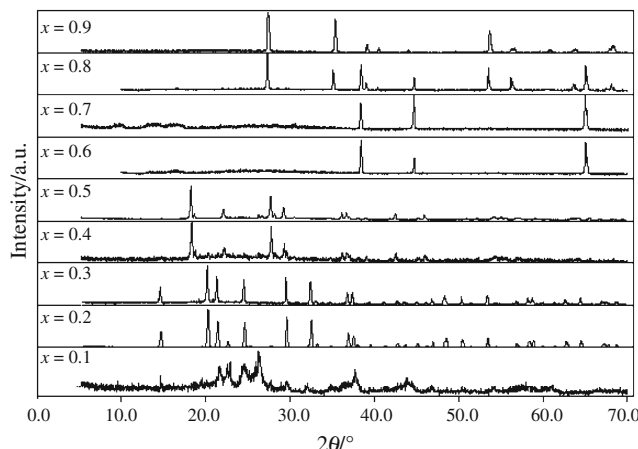


Fig. 6 XRD of batches B after heating at 900 °C

Table 3 Phase analysis of the samples heated at 900 °C

x	Phases	ICDD File
0.9	SbVO ₄	16-0600
0.8	SbVO ₄	16-0600
0.7	VO (V ₂ O ₂)	77-2173
0.6	VO (V ₂ O ₂)	77-2173
0.5	SbOPO ₄	40-0037
0.4	SbOPO ₄	40-0037
0.3	SbP ₅ O ₁₄	36-0006
0.2	SbP ₅ O ₁₄	36-0006
0.1	SbPO ₄	23-0793

Second group: $x = 0.6$ and 0.7

In this case, the compound identified was vanadium monoxide VO, of cubic system with lattice parameter $a = 4.06 \text{ Å}$ (ICDD 77-2173). As the valence state of vanadium in this compound is formally V²⁺, at the first glance this shift would seem very sharp. However, if one represents this compound as a dimer V₂O₂, the difference between V₂O₃ and V₂O₂ will no longer seem so remarkable. On the other hand, the region between V₂O₃ and V₂O₂ is characterized by a series of continuous solid solution of the composition V_nO_{2n-1} [18]. This suggests that the compositions belonging to the second group are, in reality, non-stoichiometric intermediate compounds with the structure of tetragonal VO. Some of them, for example, V₂O_{2.30} have been earlier described and characterized [19].

Third group: $x = 0.4$ and 0.5

The XRD patterns (Fig. 6) show the existence of a single crystalline phase which is the SbOPO₄ belonging monoclinic system with parameters $a = 6.791$; $b = 8.033$; $c = 7.046 \text{ Å}$ and $\beta = 115.50^\circ$ (ICDD 40-0037). This

compound contains pentavalent antimony, meaning that vanadium necessarily should be present in its lower oxidation state, that is V³⁺.

Fourth group: $x = 0.2$ and 0.3

The XRD patterns of the samples in this group are identical (Fig. 6). The only crystalline phase present is a compound identified as aforementioned antimony ultraphosphate, SbP₅O₁₄, isostructural with a well known bismuth ultraphosphate [20]. The formation can be due to the condensation of antimony polyphosphate (2 mol) with the consequent re-grouping into one mol of crystalline ultraphosphate and one mol of vitreous orthophosphate:



Fifth group $x = 0.1$

The diffractogram of batch B with $x = 0.1$ (Fig. 6) is easily identified as belonging to monoclinic antimony orthophosphate SbPO₄ with lattice parameters $a = 5.086$; $b = 6.755$; $c = 4.725 \text{ Å}$, and $\beta = 94.66^\circ$ (ICDD 23-0793).

The crystalline phases identified in batches B after heating at 900 °C for all values of x studied are summarized in Table 3.

Conclusions

Thermogravimetric analysis and X-ray diffraction data show that the interaction between ammonium metavanadate and antimony oxide leads to the formation of antimony metavanadate, Sb(VO₃)₃. The compound crystallizes in monoclinic system with lattice parameters: $a = 17.150$; $b = 15.940$; $c = 14.600 \text{ Å}$ and $\beta = 90.50^\circ$. The processes occurring in the system $x\text{NH}_4\text{VO}_3 + (1 - x)(\text{NH}_4)_2\text{HPO}_4 + \text{Sb}_2\text{O}_3$ also include the formation of Sb(VO₃)₃, SbPO₄ (at 500 °C) as well as SbVO₄, SbOPO₄, VO, and SbP₅O₁₄ (at 900 °C) showing the importance of redox reactions. No solid solutions containing simultaneously PO₄⁻³ and VO₄⁻³ ions have been found.

Acknowledgements This work was supported by CAPES and CNPq (Brazilian agencies). The authors are indebted to Microscopy Electronic Center (CME-UFRGS) for the SEM and EDS analyses.

References

- Talledo A, Granqvist CG. Electrochromic vanadium-pentoxyde-based films-structural, electrochemical, and optical-properties. *J Appl Phys*. 1995;77(9):4655–66.
- Julien C, Haro-Poniatowski E, Camacho-Lopez MA, Escobar-Alarcon L, Jimenez-Jarquin J. Growth of V₂O₅ thin films by

- pulsed laser deposition and their applications in lithium micro-batteries. *Mat Sci Eng B Solid*. 1999;65(3):170–6.
- 3. Fei HL, Zhou HJ, Wang JG, Sun PC, Ding DT, Chen TH. Synthesis of hollow V₂O₅ microspheres and application to photocatalysis. *Solid State Sci*. 2008;10(10):1276–84.
 - 4. Grigorieva AV, Tarasov AB, Goodilin EA, Badalyan SM, Rumyantseva MN, Gaskov AM, et al. Sensor properties of vanadium oxide nanotubes. *Mendeleev Comm*. 2008;18(1):6–7.
 - 5. Nilsson J, Landa-Cánovas A, Hansen S, Andersson A. Catalysis and structure of the SbVO₄/Sb₂O₄ system for propane ammoxidation. *Catal Today*. 1997;33(1–3):97–108.
 - 6. Patrina IB, Ioffe VA. Electrical properties of vanadium pentoxide. *Sov Phys Solid State, USSR*. 1965;6(11):2581.
 - 7. Schuer H, Klemm W. Note on VSbO₄. *Z Anorg Allg Chem*. 1973;395(2–3):287–90.
 - 8. Duquenoy G, Josien FA, Livage J, Michaud M. Demonstration of a compound of mixed valences in the Sb₂O₃–V₂O₅ system. *Rev de Chim Miner*. 1981;18(4):344–54.
 - 9. Filipek E, Piz M. The reactivity of SbVO₅ with T-Nb₂O₅ in solid state in air. *J Therm Anal Calorim*. 2010;101(2):417–53.
 - 10. Melnikov P, dos Santos FJ, Santagnelli SB, Secco MAC, Guimaraes WR, Delben A, et al. Mechanism of the formation and properties of antimony polyphosphate. *J Therm Anal Calorim*. 2005;81(1):45–9.
 - 11. Shimizu A, Watanabe T, Inagaki M. Single-crystal study of topotactic changes between NH₄VO₃ and V₂O₅. *J Mater Chem*. 1994;4(9):1475–8.
 - 12. Taniguchi M, Ingraham TR. Mechanism of thermal decomposition of ammonium metavanadate. *Can J Chem-Rev Can Chim*. 1964;42(11):2467–73.
 - 13. Khulbe KC, Mann RS. Thermal-decomposition of ammonium metavanadate. *Can J Chem Rev Can Chim*. 1975;53(19):2917–21.
 - 14. Durif A. Crystal chemistry of condensed phosphates. New York: Hing Corporation; 1995.
 - 15. Melnikov P, Guirardi AL, Secco MAC, de Aguiar EN. Study of the trivalent elements polyphosphates by thermal analysis. *J Therm Anal Calorim*. 2008;94(1):163–7.
 - 16. Melnikov P, dos Santos HWL, Gonçalves RV. Thermal behavior of the mixed composition x Sb₂O₃–(1 – x)Bi₂O₃–6(NH₄)₂HPO₄. *J Therm Anal Calorim*. 2009;101(3):907–11.
 - 17. Irigoyen B, Juan A, Larrondo S, Amadeo N. The electronic structure of vanadium antimonate: a theoretical study. *Catal Today*. 2005;107–108:40–5.
 - 18. Greenwood NN, Earnshaw A. Chemistry of the elements. 2nd ed. Oxford: Elsevier; 1998.
 - 19. Schwingenschlogl U, Eyert V. The vanadium Magneli phases V(n)O(2n – 1). *Ann Phys-Berlin*. 2004;13(9):475–510.
 - 20. Hilmer N, Chudinova NN, Jost KH. Condensed bismuth phosphates. *Inorg Mater*. 1978;14(8):1178–84.